A Variational Method for Computing Surface Heat Fluxes from ARM Surface Energy and Radiation Balance Systems

QIN XU AND CHONG-JIAN QIU

Cooperative Institute for Mesoscale Meteorological Studies, University of Oklahoma, Norman, Oklahoma

(Manuscript received 18 March 1996, in final form 6 June 1996)

ABSTRACT

A variational method is developed to compute surface fluxes of sensible and latent heat from observed wind, temperature, humidity, and surface energy and radiation budget by the surface energy and radiation balance systems (SERBS). In comparison with the conventional Bowen ratio energy balance method and profile method, the new method makes better and more complete use of the information provided by the SERBS measurements, and by the surface energy balance equation and the similarity profile equations. Tested with the data collected at the Oklahoma Atmospheric Radiation Measurement Cloud and Radiation Testbed central station, the method is found to be more reliable and accurate than the two conventional methods.

1. Introduction

The surface energy and radiation balance system (SERBS) measures near-surface wind, vertical gradients of temperature and water vapor pressure, and surface energy budget. Using these observations, surface fluxes of sensible and latent heat can be computed by the Bowen ratio energy balance (BREB) method (Fritschen and Simpson 1989). However, the BREB method becomes computationally unstable and produces spurious large values in the computed fluxes when the Bowen ratio is in the vicinity of -1. In addition, the BREB method does not make full use of the information provided by the similarity law for turbulent flow in the surface layer. On the other hand, the profile method uses the equations of the similarity law to compute surface fluxes of sensible and latent heat from the atmospheric measurements in the surface layer (Panofsky and Dutton 1984), but it does not use the information provided by the surface energy budget measurements. Since neither of the above methods uses the complete information provided by the SERBS measurements and the similarity law, a variational method is developed in this paper to make full use of the information. The new method is applied to the SERBS data collected during 10–19 July 1994 at the Oklahoma Atmospheric Radiation Measurement Cloud and Radiation Testbed (ARM-CART) central station (Stokes and Schwartz 1994). The SERBS data are described in the next section with a brief review of the BREB method and the profile method. The variational method is introduced in section 3. The method is tested with the SERBS data in section 4, and the results are compared with those computed by the BREB method and the profile method. Conclusions follow in section 4.

Corresponding author address: Dr. Qin Xu, Chief Scientist of CAPS, Senior Research Scientist of CIMMS, University of Oklahoma, 100 East Boyd, Room 1110, Norman, OK 73019.
E-mail: ginxu@uoknor.edu

2. Data and conventional methods

a. Data

In this paper, we use the data measured by the surface energy and radiation balance system during 10–19 July 1994 at the Oklahoma ARM-CART central station (36.61°N, 97.49°W, altitude 315 m). The ground surface around the station is flat and covered with short grasses. The data were collected every 30 min, so there are 480 time levels of observations for the selected 10-day period. The SERBS makes the following measurements: u is the horizontal wind speed at 3.4 m AGL, $\Delta\theta_1$ is the temperature difference between 0.96 and 1.96 m (inside the temperature sensor chamber), $\Delta\theta_2$ is the temperature difference between 0.96 and 1.96 m (inside the humidity sensor chamber), Δe is the water vapor pressure difference between 0.96 and 1.96 m, G is the soil heat flux at the surface, and R is the net radiative flux (near the surface). Here, $\Delta\theta_1$ is measured inside the temperature sensor chamber, $\Delta\theta_2$ is measured together with the relative humidity inside the humidity sensor chamber, and the water vapor pressure difference Δe is calculated from the relative humidity and temperature measurements inside the humidity sensor chamber (at 0.96 and 1.96 m) together with the measurement of the atmospheric pressure p at the surface level. The measurement resolutions are ± 0.1 m s^{-1} for u, ± 0.01 K for $\Delta\theta_1$ and $\Delta\theta_2$, ± 0.01 mb for Δe (or $\pm 0.6 \times 10^{-5}$ for Δq), and ± 0.1 W m^{-2} for

G and R. In this paper, the water vapor pressure difference is converted into the specific humidity difference by $\Delta q \approx 0.622\Delta e/p$.

b. Profile method

According to the Monin–Obukhov similarity theory (see Businger et al. 1971; Yaglom 1977; McBean 1979), the vertical profiles of wind, temperature, and specific humidity for turbulent flows in the surface layer can be described by the following equations:

$$u(z) = \frac{u_*}{\kappa}\left[\ln\left(\frac{z}{z_0}\right) - \Psi_M\left(\frac{z}{L}\right) + \Psi_M\left(\frac{z_0}{L}\right)\right], \quad (1)$$

$$\Delta\theta = \theta(z_2) - \theta(z_1) = \frac{\theta_*}{\kappa}\left[\ln\left(\frac{z_2}{z_1}\right) - \Psi_H\left(\frac{z_2}{L}\right) + \Psi_H\left(\frac{z_1}{L}\right)\right], \quad (2)$$

$$\Delta q = q(z_2) - q(z_1) = \frac{q_*}{\kappa}\left[\ln\left(\frac{z_2}{z_1}\right) - \Psi_Q\left(\frac{z_2}{L}\right) + \Psi_Q\left(\frac{z_1}{L}\right)\right], \quad (3)$$

where u_* is the friction velocity defined by $u_*^2 \equiv \tau/\rho$ in association with the wind stress τ and air density ρ; z_0 is the surface roughness length; $\kappa \approx 0.4$ is the von Kármán constant; θ_* is the flux temperature scale; q_* is the flux specific humidity scale; Ψ_M, Ψ_H, and Ψ_Q are the stability functions [see (6)–(9)]; $L = u_*^2 T/\kappa g\theta_*$ is the Obukhov length; $T = [\theta(z_1) + \theta(z_2)]/2$; and g is the acceleration of gravity. The flux temperature scale is related to the sensible heat flux by

$$H = -c_P\rho u_*\theta_*, \quad (4)$$

where c_P is the specific heat at constant pressure. The flux specific humidity scale q_* is related to the latent heat flux by

$$\lambda E = -\lambda\rho u_* q_*, \quad (5)$$

where λ is the latent heat of evaporation.

Different forms of stability functions have been derived and used in the literature. According to the recent review of Hogstrom (1988), the early formulations obtained by Paulson (1970), Dyer and Hicks (1970), and Hicks (1976) are still good approximations for an unstable surface layer. Their stability functions can be used in this paper for the case of unstable stratification ($\theta_* < 0$ or $L < 0$), and the formulations are given by

$$\Psi_M = 2\ln\left(\frac{1+x}{2}\right) + \ln\left(\frac{1+x^2}{2}\right) - 2\tan^{-1}(x) + \frac{\pi}{2}, \quad (6)$$

$$\Psi_{H,Q} = 2\ln\left(\frac{1+x^2}{2}\right), \quad (7)$$

where

$$x = \left(\frac{1-16z}{L}\right)^{1/4} = \left(1 - \frac{16z\kappa g\theta_*}{Tu_*^2}\right)^{1/4}.$$

For the case of stable or very stable stratification ($\theta_* > 0$ or $L > 0$), we use the stability functions suggested by Holtslag and DeBruin (1988) and Beljaars and Holtslag (1991); that is,

$$-\Psi_M = a\frac{z}{L} + b\left(\frac{z}{L} - \frac{c}{d}\right)\exp\left(-d\frac{z}{L}\right) + \frac{bc}{d}, \quad (8)$$

$$-\Psi_{H,Q} = \left(1 + \frac{2}{3}\frac{az}{L}\right)^{3/2} + b\left(\frac{z}{L} - \frac{c}{d}\right)\exp\left(-d\frac{z}{L}\right) + \frac{bc}{d} - 1, \quad (9)$$

where $a = 1$, $b = 0.667$, $c = 5$, and $d = 0.35$. In (7) and (9), $\Psi_H = \Psi_Q$ is assumed.

On the left-hand side of (1)–(3), the horizontal wind speed, temperature difference, and specific humidity difference can be directly determined by the SERBS measurements. On the right-hand side of (1)–(3), the roughness length can be estimated as an external parameter (see section 4a), so there are three unknowns in (1)–(3): the friction velocity u_*, the flux temperature scale θ_*, and the flux specific humidity scale q_*. Since these three unknowns can be computed by an iterative procedure from (1)–(3), sensible heat flux and latent heat flux can be estimated by (4) and (5). This is the profile method (Nieuwstadt 1978; McBean 1979). Clearly, this method does not use the surface energy budget measurements (G and R in section 2a). Due to the approximations used in (1)–(9) and limited accuracy in the observational data, the total flux of $H + \lambda E$ computed by the profile method could be significantly different from the observed value of $G + R$ and thus violate the surface energy balance [see (10)].

c. BREB method

The Bowen ratio energy balance method has been reviewed by many and tested in various agricultural settings (Tanner 1960; Fritschen 1965; Pruitt and Lourence 1968). The method uses the SERBS measurements (see section 2a) together with the following surface energy balance equation:

$$H + \lambda E = R + G, \quad (10)$$

where G is the soil heat flux and R is the net radiative flux (see section 2a). By introducing the Bowen ratio $B = H/\lambda E$, this balance equation can be rewritten as

$$\lambda E = \frac{R+G}{1+B}. \quad (11)$$

Substituting (2) and (3) into the ratio between (4) and (5), and using $\Psi_H = \Psi_Q$ [as assumed in (7) and (9)], we obtain

$$B = \frac{c_P \Delta\theta}{\lambda \Delta q}. \tag{12}$$

As described in section 2a, $\Delta\theta$ (either $\Delta\theta_1$ or $\Delta\theta_2$), $\Delta q = 0.622\Delta e/p$, R, and G are all directly measured, so we can estimate the Bowen ratio from (12) and then compute the latent heat flux from (11) and obtain the sensible heat flux from $H = \lambda EB$.

The BREB method uses all the SERBS measurements listed in section 2a and has generally been considered the most conservative and reliable all-weather technique for flux computations (Priestley and Taylor 1972; Fritschen and Simpson 1989). However, it is also well known that the BREB method will become computationally unstable when the Bowen ratio is in the vicinity of -1. In this case, as we can see from (11), a small observational error in $R + G$ or B will cause very large errors in the computed fluxes. To eliminate this problem, a variational method is developed in the next section.

3. Variational method

The profile method uses all the equations of the similarity law, but it does not use the surface energy budget measurements. The BREB method uses all the SERBS measurements, but it does not use all the information in (1)–(9) provided by the similarity law, although (12) is derived from the ratio between (2) and (3) [or (4) and (5)]. To make full use of the SERBS measurements and the similarity law, we need to combine the above two methods into a variational method. The objective is to find the optimal estimates of (u_*, θ_*, q_*) that minimize the following cost function:

$$J = \frac{1}{2}\left[w_u(u - u^{\text{ob}})^2 + \sum_{i=1}^{2} w_i(\Delta\theta - \Delta\theta_i^{\text{ob}})^2 + w_q(\Delta q - \Delta q^{\text{ob}})^2 + w_r\delta^2 \right], \tag{13}$$

where u, $\Delta\theta$, and Δq are functions of (u_*, θ_*, q_*) given by (1)–(3); u^{ob}, $\Delta\theta_i{}^{\text{ob}}$ ($i = 1, 2$), and Δq^{ob} are the observed wind, temperature difference, and specific humidity difference, respectively (see section 2a); and

$$\delta = R + G - H - \lambda E. \tag{14}$$

Here, R and G are given observationally (see section 2a), and H and λE are computed as functions of (u_*, θ_*, q_*) from (4) and (5), so δ measures the mismatch between the computed $H + \lambda E$ and observed $R + G$ under the constraint of the surface energy balance equation (10). The first three terms on the right-hand side of (13) measure the mismatches between the computed and observed winds, temperature differences, and humidity differences, respectively. All these terms should be inversely weighted by their respective observation error variances, so the minimum point of J gives the optimal estimates of (u_*, θ_*, q_*) (Lorenc 1986; Daley 1991). In this paper, the following estimated values are used for the weights: $w_u = 10\ \text{m}^{-2}\ \text{s}^2$, $w_1 = 100\ \text{K}^{-2}$, $w_2 = w_1/4$, $w_q = 10^8$, and $w_r = 10^{-4}\ \text{W}^{-2}\ \text{m}^4$. Here, by choosing $w_2 = w_1/4$, $\Delta\theta_2$ is used as a supplemental data source that is independent of $\Delta\theta_1$, although $\Delta\theta_2$ is measured in nearly the same way as $\Delta\theta_1$ and only $\Delta\theta_1$ is used by the BREB method to compute the Bowen ration in (12). If $w_2 = 0$ and $w_r = 0$ are chosen, then the number of constraints used in (13) reduces from 5 to 3. In this case, the number of constraints (or equations) equals the number of unknowns, and the variational method reduces to the profile method. At the minimum point of J, the three gradient components of J with respect to the unknown variables (u_*, θ_*, q_*) should be zero:

$$\frac{\partial J}{\partial u_*} = \frac{\partial J}{\partial \theta_*} = \frac{\partial J}{\partial q_*} = 0. \tag{15}$$

To search for the minimum, it is necessary to compute the gradient components. The analytical expressions of the gradient components in (14) can be derived from (1)–(9), and the detailed formulations are given in the appendix. With the gradient formulations, the memoryless quasi-Newton algorithm (Liu and Nocedal 1988) can be conveniently used to find the minimum of J. The iterative procedure consists of the following basic steps.

1) Start from initial guesses of the unknowns, say, $u_* = 0.1\ \text{m s}^{-1}$, $\theta_* = 0$, and $q_* = 0$.
2) Compute u, $\Delta\theta$, and Δq from (1)–(3), and compute δ from (14) by using (4) and (5).
3) Calculate the cost function J in (13) and its three gradient components by using (A1)–(A3).
4) If the convergence criterion is satisfied ($|\nabla J| \le 10^{-4}$), then the expected estimates (u_*, θ_*, q_*) are reached at the minimum of the cost function. Otherwise, determine a search direction based on the gradients and the search directions of previous iterations.
5) Determine the search step size and find the minimum of J along the search direction, obtain the new estimates of (u_*, θ_*, q_*), and return to step 2.

In the algorithm the step size is approximately determined by fitting a cubic curve through a number of points along the line of the search. To improve the convergence rate of iteration, (u_*, θ_*, q_*) should be properly scaled to make the supersurface of the cost function more spherical, or, say, less elliptical (Moore 1991; Xu et al. 1994). In this paper, (u_*, θ_*, q_*) are scaled by (1 m s^{-1}, 0.5 K, 0.5×10^{-3}). The convergence criterion is $|\nabla J| \le 10^{-4}$, where ∇J represents the gradient of J with respect to the scaled (u_*, θ_*, q_*). With this criterion, the minimization procedure is found to converge within 8–22 iterations. The computational code contains about 500 lines and is very efficient. It takes only 20 s on a workstation to produce all the results (every 30 min for the 10-day period) presented in this paper.

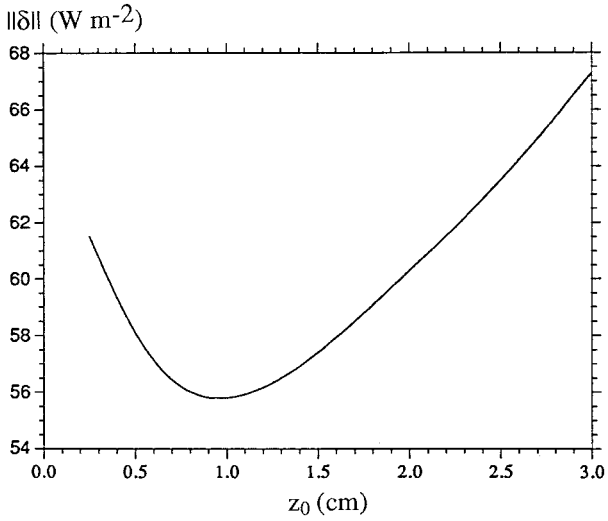

FIG. 1. The variation of $\|\delta\|$ as a function of z_0. Here, $\|\delta\|$ is the rms value of δ (see section 4a) and δ is given by (14), with $H + \lambda E$ computed by the profile method.

4. Results and discussions

The two conventional (BREB and profile) methods and the new variational method are tested with the SERBS data collected every 30 min at the Oklahoma ARM-CART central station during 10–19 July 1994. The detailed results are examined and intercompared in the following subsections.

a. Estimate of surface roughness length

The surface roughness length z_0 is an important parameter for the profile method and variational method. The local roughness length (over an area of 1–10 km^2) is related to the roughness characteristics of the surface. Since the terrain around the Oklahoma ARM-CART central station is flat and covered by short grasses, a crude estimate of z_0 can be made in the range from 0.005 to 0.03 m (Wieringa 1981). This estimated range of z_0 can be improved by using the information provided by the surface energy budget measurements. The details are as follows.

Assume that z_0 does not change during the selected period (10 days). For a selected value of z_0, the sensible and latent heat fluxes can be computed by the profile method. Substituting these computed values of H and λE, together with the observed values of R and G, into (14) gives the residual value of δ. For total $N = 480$ time levels of observations during the selected period (10–19 July 1994), the rms value of δ is computed by $\|\delta\| = (N^{-1} \sum_{n=1}^{N} \delta_n^2)^{1/2}$, and the result is plotted as a function of z_0 in Fig. 1. As shown, $\|\delta\|$ has a minimum around $z_0 = 0.01$ m, suggesting that $z_0 = 0.01$ m should be used in order to closely satisfy the surface energy budget. This estimated value is used in this paper, which is the same as the value obtained by Beljaars (1988) for short grass from the data collected during the Cabauw field experiment.

b. Comparisons of different methods

Because direct measurements of fluxes are not available, the computed heat fluxes cannot be precisely eval-

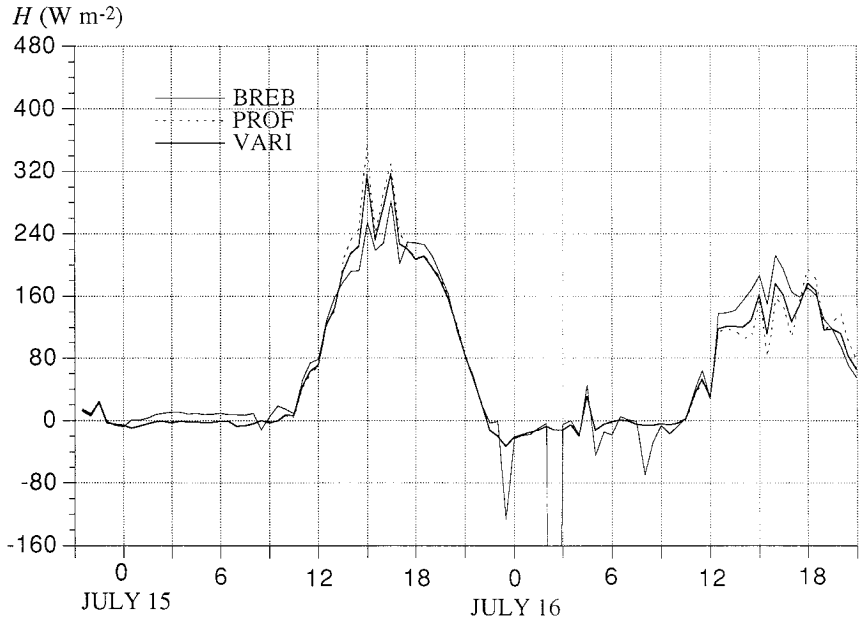

FIG. 2. Time variation of sensible heat fluxes computed by the three methods for the 48-h period (local time) from 15 to 16 July 1994. The thin solid line is for the BREB method, the dashed line is for the profile (PROF) method, and the thick solid line is for the variational (VARI) method.

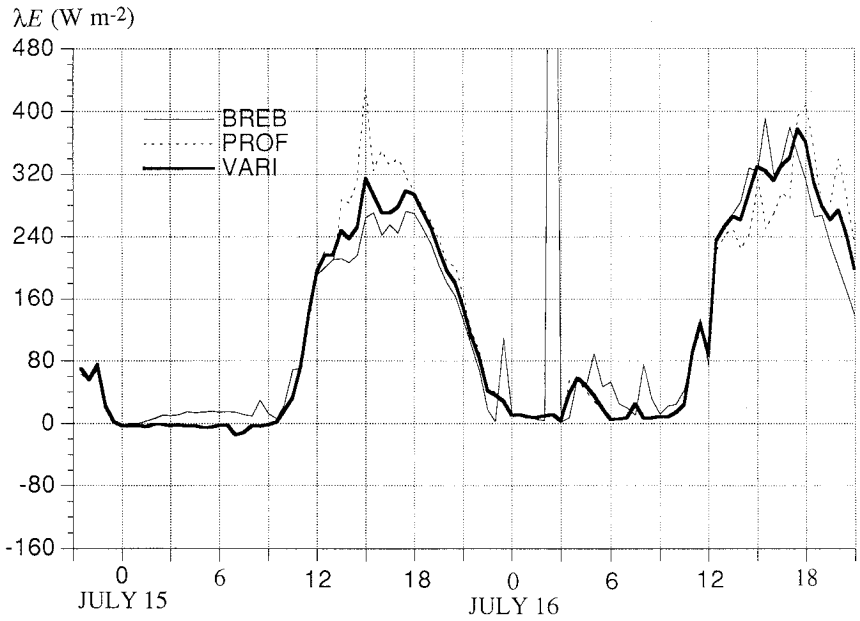

FIG. 3. As in Fig. 5 but for latent heat fluxes.

uated. A qualitative evaluation, however, can be made by intercomparisons of the results obtained by the three methods. The computed sensible and latent heat fluxes are shown (for 15–16 July only) in Figs. 2 and 3, respectively. Two problems are seen for the BREB method. 1) The computed fluxes jump and cause spurious spikes when the Bowen ratio becomes close to -1 (in the nighttime between 2000 LT 15 July and 0600 LT 16 July). 2) The computed sensible (or latent) heat flux sometimes (for example, during 0000–0430 LT 15 July) has a sign opposite to the observed vertical gradient of temperature (or humidity). These problems are fairly well known for the BREB method. The profile method and the variational method do not have these problems.

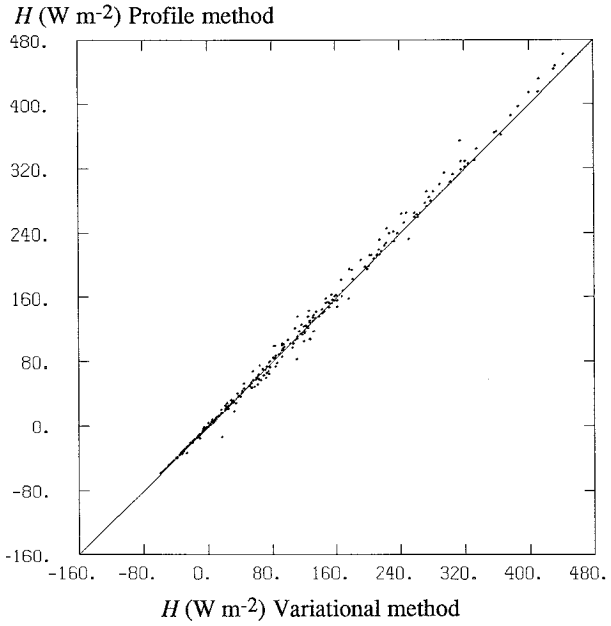

Fig. 4. Correlation diagram for sensible heat fluxes computed by the profile and variational methods.

In the daytime, the fluxes computed by the profile method show relatively large fluctuations and do not closely match the observed value of $R + G$ as required by the surface energy balance equation (10). The mismatch between the computed total flux $H + \lambda E$ and the observed value of $R + G$ can be measured by $\|\delta\|$. The indicated mismatch is $\|\delta\| \geq 56$ W m^{-2} for the profile method (see Fig. 1) and reduces to $\|\delta\| = 15$ W m^{-2} for the variational method (not shown). During most of the 10-day period, the fluxes computed by the variational method are between those computed by the BREB method and by the profile method.

To show the overall comparisons, each pair of flux values computed by two different methods is plotted as a point in their respective correlation diagrams (Figs. 4–7). Each correlation diagram contains 480 points corresponding to the $N = 480$ time levels of observations during the selected period (10–19 July 1994). In Fig. 4 the profile method is compared with the variational method. As shown, the correlation points are mostly distributed above the diagonal line when the sensible heat flux is positive and large. Thus, in comparison with the variational method, the profile method tends to overestimate sensible heat flux when the stratification is unstable. The BREB method is compared with the variational method in Fig. 5, where a number of points show large vertical deviations from the diagonal line. These large deviations are caused by the spurious large fluxes computed by the BREB method for those cases in which

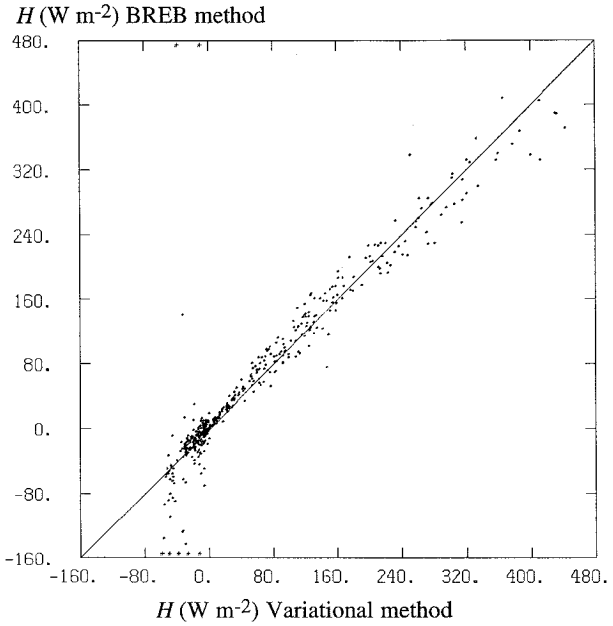

FIG. 5. As in Fig. 4 but for the BREB method versus the variational method. Points with large positive (or negative) fluxes computed by the BREB method beyond 480 (or −160) W m^{-2} are plotted along the top (or bottom) boundary.

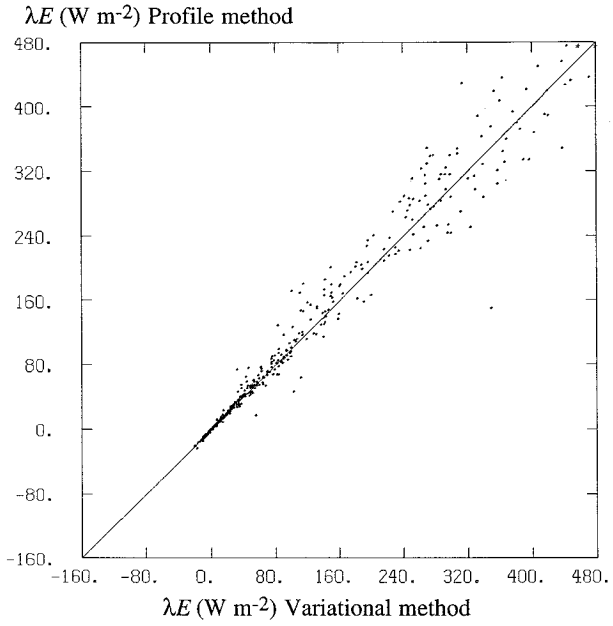

FIG. 6. As in Fig. 4 but for latent heat fluxes.

the stratification is very stable and the Bowen ratio is close to −1. Clearly, when the Bowen ratio becomes close to −1, the BREB method fails but the variational method still works well. Similar results are obtained for the computed latent heat fluxes in Figs. 6 and 7.

c. *Sensitivity experiments*

The relative advantages and disadvantages of the three methods can be also evaluated by examining the sensitivities of their computed fluxes with respect to data errors. For this purpose, additional ''data errors'' of 0.5 m s^{-1}, 0.05 K, 0.1×10^{-4}, and 5.0 W m^{-2} are added to the observed wind at 3.4 m, temperature at 0.96 m, specific humidity at 0.96 m, and the observed values of $R + G$, respectively (for the $N = 480$ time levels). Five different combinations of these data errors are listed in Table 1. Fluxes are computed by each method with and without the data errors. The rms differences between the computed fluxes with and without the data errors are listed in Table 1 for each combination and each method. As shown, among the three methods, the variational method is most insensitive to data errors, while the BREB method is most sensitive to data errors.

The high sensitivity of the BREB method is largely caused by its computational instability when the Bowen ratio becomes close to −1, or, say, when $|B + 1|$ becomes close to zero. As shown in Table 2, the sensitivity of the BREB method can be reduced if the computations are restricted by $|B + 1| > \epsilon$, or, say, if the computations are performed only for those cases in which $|B + 1| > \epsilon$. However, the sensitivity of the BREB method cannot be reduced to the level of the variational method even when the computations are restricted by $|B + 1| > 0.25$ (with 8.5% cases excluded). Thus, although some alternate methods were previously proposed to substitute the BREB method in case of $|B + 1| < \epsilon \ll 1$ [see, for example, section 6 of Fritschen and Simpson (1989)], there is not a clear way to select the threshold value ϵ for an alternate method to be used. The variational method proposed in

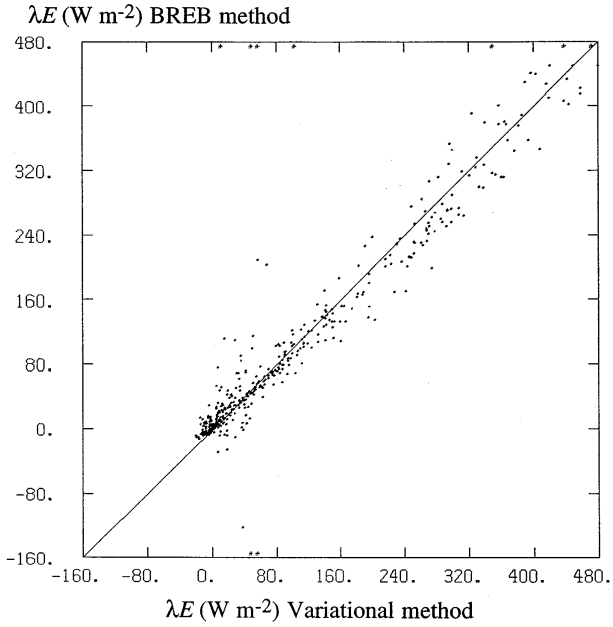

FIG. 7. As in Fig. 5 but for latent heat fluxes.

TABLE 1. Sensitivities of computed fluxes with respect to data errors. Here, B, P, and V denote the BREB and the profile and variational methods, respectively.

Data errors				rms errors in computed fluxes					
				H (W m^{-2})			λE (W m^{-2})		
u (m s^{-1})	$-\Delta\theta$ (K)	$-\Delta q$ (10^{-4})	$R+G$ (W m^{-2})	B	P	V	B	P	V
0.5	0.0	0.0	0.0	0.0	10.8	5.4	0.0	10.7	10.5
0.0	0.05	0.0	0.0	485.9	15.1	8.5	485.9	7.0	4.7
0.0	0.0	0.1	0.0	91.1	0.0	4.4	91.1	8.2	8.2
0.0	0.0	0.0	5.0	14.4	0.0	1.0	14.1	0.0	2.0
0.5	0.05	0.1	5.0	156.9	12.5	9.3	156.9	15.8	8.6

this paper provides a rational resolution to the problem caused by small $|B + 1|$ in the BREB method.

5. Conclusions

In this paper, two conventional methods, the profile method and the Bowen ratio energy balance method, are reviewed for their relative advantages and disadvantages in computing surface fluxes of sensible heat and latent heat. Briefly, the profile method uses the full information provided by the similarity law for turbulent flow in the surface layer, but it does not use the surface energy budget measurements, while the BREB method does the opposite. Since neither of the conventional methods uses the complete information provided by the measurements and the similarity law, a variational method is developed in this paper to combine the advantages of the two conventional methods.

Tested with the data collected by the surface energy and radiation balance systems during 10–19 July 1994 at the ARM central station, the variational method is found to be more reliable and less sensitive to data errors than the two conventional methods. In particular, the results show that the BREB method becomes computationally unstable and causes spurious spikes in the computed fluxes when the Bowen ratio is in the vicinity of -1. This problem is fairly well known and is now solved by the variational method in a more rational way than the previously suggested alternative methods. The variational method is also more accurate than the profile method in terms of satisfying the surface energy balance and matching the observed soil heat flux and net radiative flux.

In this paper, the variational method is evaluated only in a relative sense with respect to the conventional BREB and profile methods. In most cases, the variational method gives fluxes somewhere in between those of the two conventional methods, and in case of a clear breakdown of any of the conventional methods, the variational method gives more weight to the information that is really useful for estimating the fluxes. The variational method will be further evaluated when direct eddy-correlation measurements of fluxes become available from the ARM data in the near future.

Although the variational method is tested with the SERBS data for 10 days under a variety of dry and wet weather conditions characterized by a very wide range of Bowen ratios (from $B \ll -1$ to $B \gg 1$), the method may become relatively inaccurate when the temperature and humidity gradients are very small or measured by the Oklahoma Mesonet (with relatively large errors). To solve this problem, the current variational method needs to be extended. In particular, the model's atmospheric layer should be coupled with a soil/vegetation layer, so that the extended method can utilize not only the atmospheric measurements but also the soil temperature and moisture measurements provided by the ARM data or the Oklahoma Mesonet data. This problem is under our investigation, and the preliminary results are very encouraging (Xu and Zhou 1996).

TABLE 2. Percentage of cases restricted by $|B + 1| > \epsilon$ and related rms errors in fluxes computed by the BREB method for restricted cases. The data errors are the same as in the last line of Table 1.

ϵ	Percentage (%)	rms errors in computed fluxes	
		H (W m^{-2})	λE (W m^{-2})
0.05	98.1	72.28	72.39
0.10	96.5	56.05	56.08
0.15	94.4	48.78	48.93
0.20	91.9	12.87	13.06
0.25	91.5	10.11	10.24

Acknowledgments. We are thankful to Michael Splitt for the ARM data support, and to Bibin Zhou and anonymous reviewers for their comments and suggestions, which improved the presentation of the results. This work is supported by the National Oceanic and Atmospheric Administration Contract NA37RJ0203, the U.S. Air Force Grant F49620-95-1-0320, and the Department of Energy ARM Program through Battelle PNL Contract 144880-A-Q1 to CIMMS, University of Oklahoma.

APPENDIX

Formulations for the Gradient Components

By using the chain rule of differentiation, the gradient components of the cost function J, defined in (13) with respect to (u_*, θ_*, q_*), are obtained as follows:

$$\frac{\partial J}{\partial u_*} = w_u(u - u^{ob})\frac{\partial u}{\partial u_*} + \sum_{i=1}^{2} w_i(\Delta\theta - \theta_i^{ob})\frac{\partial \Delta\theta}{\partial u_*} + w_q(\Delta q - \Delta q^{ob})\frac{\partial \Delta q}{\partial u_*} + w_r\delta\frac{\partial \delta}{\partial u_*}, \quad \text{(A1)}$$

$$\frac{\partial J}{\partial \theta_*} = w_u(u - u^{ob})\frac{\partial u}{\partial \theta_*} + \sum_{i=1}^{2} w_i(\Delta\theta - \theta_i^{ob})\frac{\partial \Delta\theta}{\partial \theta_*} + w_q(\Delta q - \Delta q^{ob})\frac{\partial \Delta q}{\partial \theta_*} + w_r\delta\frac{\partial \delta}{\partial \theta_*}, \quad \text{(A2)}$$

$$\frac{\partial J}{\partial q_*} = w_q(\Delta q - \Delta q^{ob})\frac{\partial \Delta q}{\partial q_*} + w_r\delta\frac{\partial \delta}{\partial q_*}, \quad \text{(A3)}$$

where

$$\frac{\partial u}{\partial u_*} = \frac{1}{\kappa}\left[\ln\left(\frac{z}{z_0}\right) - \Psi_M\left(\frac{z}{L}\right) + \Psi_M\left(\frac{z_0}{L}\right)\right] - \frac{u_*}{\kappa}\left[\frac{\partial \Psi_M(z/L)}{\partial u_*} - \frac{\partial \Psi_M(z_0/L)}{\partial u_*}\right],$$

$$\frac{\partial \Delta\theta}{\partial u_*} = -\frac{\theta_*}{\kappa}\left[\frac{\partial \Psi_M(z_2/L)}{\partial u_*} - \frac{\partial \Psi_H(z_1/L)}{\partial u_*}\right],$$

$$\frac{\partial \Delta q}{\partial u_*} = -\frac{q_*}{\kappa}\left[\frac{\partial \Psi_Q(z_2/L)}{\partial u_*} - \frac{\partial \Psi_Q(z_1/L)}{\partial u_*}\right],$$

$$\frac{\partial u}{\partial \theta_*} = -\frac{u_*}{\kappa}\left[\frac{\partial \Psi_M(z/L)}{\partial \theta_*} - \frac{\partial \Psi_M(z_0/L)}{\partial \theta_*}\right],$$

$$\frac{\partial \Delta\theta}{\partial \theta_*} = \frac{1}{\kappa}\left[\ln\left(\frac{z_2}{z_1}\right) - \Psi_H\left(\frac{z_2}{L}\right) + \Psi_H\left(\frac{z_1}{L}\right)\right] - \frac{\theta_*}{\kappa}\left[\frac{\partial \Psi_H(z_2/L)}{\partial \theta_*} - \frac{\partial \Psi_H(z_1/L)}{\partial \theta_*}\right],$$

$$\frac{\partial \Delta q}{\partial \theta_*} = -\frac{q_*}{\kappa}\left[\frac{\partial \Psi_Q(z_2/L)}{\partial \theta_*} - \frac{\partial \Psi_Q(z_1/L)}{\partial \theta_*}\right],$$

$$\frac{\partial \Delta q}{\partial q_*} = \frac{1}{\kappa}\left[\ln\left(\frac{z_2}{z_1}\right) - \Psi_Q\left(\frac{z_2}{L}\right) + \Psi_Q\left(\frac{z_1}{L}\right)\right],$$

$$\frac{\partial \delta}{\partial u_*} = -\rho(c_p\theta_* + \lambda q_*),$$

$$\frac{\partial \delta}{\partial \theta_*} = -\rho c_p u_*,$$

$$\frac{\partial \delta}{\partial q_*} = -\rho\lambda u_*.$$

The stability functions Ψ_M, Ψ_H, and Ψ_Q are given by (6) and (7) for an unstable stratification and by (8) and (9) for a stable stratification. Accordingly, the gradient components of the stability functions are given, for an unstable stratification, by

$$\frac{\partial \Psi_M}{\partial x} = 2\left(\frac{1}{1 + x} + \frac{x - 1}{1 + x^2}\right),$$

$$\frac{\partial \Psi_{H,Q}}{\partial x} = \frac{4x}{1 + x^2},$$

$$\frac{\partial x}{\partial u_*} = \frac{8z\kappa g\theta_*}{Tu_*^3}x^{-3},$$

$$\frac{\partial x}{\partial \theta_*} = \frac{-4z\kappa g}{Tu_*^2}x^{-3},$$

where $x = (1 - 16z/L)^{1/4} = (1 - 16z\kappa g\theta_*/Tu_*^2)^{1/4}$ is the same as defined in (6) and (7). For a stable stratification, the gradient components of the stability functions are given by

$$\frac{\partial \Psi_M}{\partial x} = -a - b\exp(-dx) + db\left(x - \frac{c}{d}\right)\exp(-dx),$$

$$\frac{\partial \Psi_{H,Q}}{\partial x} = -z\left(1 + \frac{2}{3}x\right)^{1/2} - b\exp(-dx) + db\left(x - \frac{c}{d}\right)\exp(-dx),$$

$$\frac{\partial x}{\partial u_*} = -\frac{2z\kappa g\theta_*}{Tu_*^3},$$

$$\frac{\partial x}{\partial \theta_*} = \frac{z\kappa g}{Tu_*^2},$$

where $x = z/L = z\kappa g\theta_*/Tu_*^2$, $a = 1$, $b = 0.667$, $c = 5$, and $d = 0.35$, as in (8) and (9).

REFERENCES

Beljaars, A. C. M., 1988: Surface fluxes in moderately complex terrain. *Proc. Eighth Symp. on Turbulence and Diffusion,* San Diego, CA, Amer. Meteor. Soc., 193–196.

——, and A. A. M. Holtslag, 1991: Flux parameterization over land surfaces for atmospheric models. *J. Appl. Meteor.*, **30,** 327–341.

Businger, J. A., J. C. Wyngaard, Y. Izumi, and E. F. Bradley, 1971: Flux profile relationships in the atmospheric surface layer. *J. Atmos. Sci.*, **28,** 181–189.

Daley, R., 1991: *Atmospheric Data Analysis.* Cambridge University Press, 457 pp.

Dyer, A. J., and B. B. Hicks, 1970: Flux gradient relationships in the constant flux layer. *Quart. J. Roy. Meteor. Soc.*, **96,** 715–721.

Fritschen, L. J., 1965: Accuracy of evapotranspiration determinations by the Bowen ratio method. *Bull. Int. Soc. Sci. Hydrol.*, **2,** 38–48.

——, and J. R. Simpson, 1989: Surface energy and radiation balance systems: General description and improvements. *J. Appl. Meteor.*, **28,** 680–689.

Hicks, B. B., 1976: Wind profile relationships from the ''Wangara'' experiments. *Quart. J. Roy. Meteor. Soc.*, **102,** 535–551.

Hogstrom, U., 1988: Nondimensional wind and temperature profiles in the atmospheric surface layer: A reevaluation. *Bound.-Layer Meteor.*, **42,** 55–78.

Holtslag, A. A. M., and H. A. R. DeBruin, 1988: Applied modeling of the nighttime surface energy balance over land. *J. Appl. Meteor.,* **27,** 689–704.

Liu, D. C., and J. Nocedal, 1988: On the limited memory BFGS method for large scale optimization. Tech. Rep. NAM03, 26 pp. [Available from Department of Electrical Engineering and Computer Science, Northwestern University, Evanston, IL 60208.]

Lorenc, A. C., 1986: Analysis methods for numerical weather prediction. *Quart. J. Roy. Meteor. Soc.,* **112,** 1177–1194.

McBean, G. A., Ed., 1979: The planetary boundary layer. Tech. Note 165, WMO-530, 201 pp.

Moore, A. M., 1991: Data assimilation in a quasi-geostrophic open-ocean model of the Gulf Stream region using the adjoint method. *J. Phys. Oceanogr.,* **21,** 398–427.

Nieuwstadt, F. T. M., 1978: The computation of the friction velocity u_* and the temperature scale T_* from temperature and wind profiles by least square methods. *Bound.-Layer Meteor.,* **14,** 235–246.

Panofsky, H. A., and J. A. Dutton, 1984: *Atmospheric Turbulence, Models and Methods for Engineering Applications.* John Wiley & Son, 397 pp.

Paulson, C. A., 1970: The mathematical representation of wind speed and temperature profiles in the unstable atmospheric surface layer. *J. Appl. Meteor.,* **9,** 856–861.

Priestley, C. H. B., and R. J. Taylor, 1972: On the assessment of surface heat flux and evaporation using large-scale parameters. *Mon. Wea. Rev.,* **100,** 81–92.

Pruitt, W. O., and F. J. Lourence, 1968: Correlation of climatological data with water requirements of crops. Water Science and Engineering Paper 9001, University of California, Davis, Davis, CA.

Stokes, G. M., and S. E. Schwartz, 1994: The Atmospheric Radiation Measurement (ARM) Program: Programmatic background and design of the Cloud and Radiation Test Bed. *Bull. Amer. Meteor. Soc.,* **75,** 1201–1221.

Tanner, C. B., 1960: Energy balance approach to evapotranspiration from crops. *Soil Sci. Soc. Amer. Proc.,* **24,** 1–9.

Wieringa, J., 1981: Estimation of mesoscale and local-scale roughness for atmospheric transport modeling. *Air Pollution Modeling and Its Applications,* C. Wispelaere, Ed., Plenum, 279–295.

Xu, Q., and B. Zhou, 1996: Computations of surface fluxes from ARM data and Mesonet data. *Proc. Sixth Atmospheric Radiation Measurement (ARM) Science Team Meeting,* San Antonio, TX, Office of Scientific and Technical Information, U.S. Department of Energy, in press.

——, C. Qiu, and J. Yu, 1994: Adjoint-method retrievals of low-altitude wind fields from single-Doppler wind data. *J. Atmos. Oceanic Technol.,* **11,** 579–585.

Yaglom, A. M., 1977: Comments on wind and temperature flux-profile relationships. *Bound.-Layer Meteor.,* **11,** 89–102.